Last-Mile Humanitarian Logistics Planning with Isolated Communities (Online Appendices)

Mahdi Noorizadegan[1], Mohammad Fattahi[1], Esmaeil Keyvanshokooh[2], Jon M. Stauffer[2]
[1]Newcastle Business School, Northumbria University, Newcastle upon Tyne, UK; m.noorizadegan@northumbria.ac.uk, mohammad.fattahi@northumbria.ac.uk.
[2]Department of Information and Operations Management, Mays Business School, Texas A&M University, College Station, TX 77843; keyvan@tamu.edu, jstauffer@mays.tamu.edu.

Appendix A: More Details on Related Works

Table A.1 Review of Main Studies on the Drone Delivery in Humanitarian Logistics Operations. In the table, we denote drone scheduling (DS), drone routing problems (DRP), drones riding with trucks (DRWT), parallel drone scheduling traveling salesman problem (PDSTSP), parallel drone scheduling vehicle routing problem (PDSVRP), and parallel drone-vehicle routing problem (PDVRP) as various drone-delivery modeling methods.

Studies	Facility Location	Fleet Size	Drone-Delivery Modeling	Uncertainty Consideration	Solution Algorithm	Coverage Difference between Isolated & Non-Isolated Communities	Real-Life Case Study
Rabta et al. (2018)	×	×	DRP	×	Optimization Software	×	×
Kim et al. (2019)	✓	✓	DS	Travel times	Benders' Decomposition	×	×
Chauhan et al. (2019)	✓	✓	DS	×	Heuristics/Meta-Heuristics	×	×
Macias et al. (2020)	✓	×	DRP	×	Heuristics/Meta-Heuristics	×	1999 Chi-Chi Earthquake in Taiwan
Chauhan et al. (2021)	✓	✓	DS	Drone Battery Consumption & Availability	Heuristics/Meta-Heuristics	×	×
Gentili et al. (2022)	✓	×	DS	×	Optimization Software	×	×
Zhu et al. (2022)	✓	✓	DS	Demand	Column & Constraint Generation Algorithm	×	×
Ghelichi et al. (2022)	✓	✓	DS	×	Heuristics/Meta-Heuristics	×	Scenarios for Hurricane-Prone Areas in the US, Central Florida
Lu et al. (2023)	×	×	DRWT	×	Heuristics/Meta-Heuristics	✓	2021 Flood in China's Henan Province
Van Steenbergen et al. (2023)	×	×	PDSVRP	Travel Times and Demand	Heuristics/Meta-Heuristics	×	2015 Earthquake in Nepal and 2018 Tsunami in Indonesia
Shadlou et al. (2023)	×	×	DS+Repair Crew Routing	×	Logic-based Benders Decomposition	×	2017 Earthquake on the Iran-Iraq Border
Yin et al. (2023)	×	×	DRWT	Travel times and Demand	Branch-and-Price-and-Cut Algorithm	✓	2008 Earthquake in Wenchuan, China
Dukkanci et al. (2023)	✓	✓	DRWT+DS	Demand and Road Distance	Scenario decomposition	×	Disaster Scenarios in Istanbul, Turkey
Faiz et al. (2024)	×	×	DRWT	Demand	Heuristics/Meta-Heuristics	✓	Disaster Scenarios in Island of Puerto Rico
Khameneh et al. (2025)	×	×	DRWT	×	Heuristics/Meta-Heuristics	×	Disaster scenarios in Hoboken, NJ, and Hopkins County, KY
Tureci-Isik et al. (2025)	✓	×	PDSVRP	Travel times	Heuristics/Meta-Heuristics	×	2011 Van Earthquake in Turkiye
Xin et al. (2025)	✓	✓	DS	Demand & Road Network	Benders' Decomposition	×	2010 Earthquake in Yushu, Qinghai, China
Yang et al. (2026)	✓	×	DRP	Facility Disruption, Demand & Delivery Deadlines	Integrated Benders' Decomposition and B&B	×	Earthquakes scenarios in Ya'an, Sichuan Province, China
Sun et al. (2026)	×	×	DRWT	×	Integrated Benders' Decomposition and B&B	✓	Typhoon Scenarios in Hong Kong Island
Our Work	✓	✓	PDVRP	Travel times and Demand	Branch-and-Price Algorithm	✓	2020 Hurricanes 2020 Eta and Iota Hurricanes

Table A.2 Summary of studies with exact solution algorithms for solving LRPs.

Studies	Heterogeneous Vehicles	Uncertainty Modeling	Fleet Size Decisions	Solution Algorithms
Baldacci et al. (2011)	✓	×	×	Lower-bounding Procedure for LRP Decomposition
Belenguer et al. (2011), Contardo et al. (2013)	×	×	×	Branch-and-Cut (B&C) Algorithm with Valid Inequalities
Contardo et al. (2014), Farham et al. (2018), Arslan (2021), Wang et al. (2022)	×	×	×	B&P Algorithm (with/without Valid Inequalities)
Arslan et al. (2021)	×	×	×	Branch-and-Cut-and-Price (BC&P) Algorithm
Çalık et al. (2021)	✓	×	×	Benders' Decomposition
Liguori et al. (2023)	×	×	×	BC&P Algorithm with Valid Inequalities
Mohamed et al. (2023)	×	Two-stage Stochastic Programming	×	Logic-based Benders' Decomposition
Wang et al. (2025)	✓	×	×	BC&P Algorithm
Our Work	✓	Distributionally Robust & CVaR-based Chance Constraints	✓	B&P Algorithm with SPPCC Pricing Problem

Appendix B: Detailed Proofs of Our Analytical Results

B.1. Proof of Proposition 1

Proposition 1 states that the pricing problem (10) can be reformulated as a shortest path problem with chance constraints. Let the updated induced subgraph $\bar{G}_k^l = (\bar{V}_k^l, \bar{E}_k^l)$ include the vertex set $\bar{V}_k^l$, consisting SA k, a replica node of SA k (denoted by k') and the set of PoDs reachable by the mobile unit l, and $\bar{E}_k^l$ is the set of edges between vertices in $\bar{V}_k^l$. Note that $c_{i,k',l} = c_{i,k,l}$ and $c_{k,k',l} = c_{k',k,l} = 0$. In the shortest path problem reformulation, SA k is the source vertex and vertex k' is the target. Let the cost associated with edge $e = (i,j) \in \bar{E}_k^l$ on the induced subgraph be defined as follows:

$$\bar{c}_{i,j,l} = \mu_j \beta_k + (\mu_{i,j,l} + \varphi_{j,l})\pi_k^l - \alpha_j(1-\omega_j) - \alpha_j^{\mathcal{D}}\omega_j \tag{15}$$

The shortest path-based pricing problem is then formulated as:

$$\text{SPPP: } \min \sum_{e \in \bar{E}_k^l} \bar{c}_{e,l}\mathrm{y}_e \tag{16a}$$

$$\text{s.t., } \sum_{j \in \delta^+(i)} \mathrm{y}_{ij} - \sum_{j \in \delta^-(i)} \mathrm{y}_{ji} = \begin{cases} 1 & \text{for } i = k \\ 0 & \text{for } i \in \bar{V}_k^l \setminus \{k, k'\} \\ -1 & \text{for } i = k' \end{cases} \tag{16b}$$

$$\inf_{\mathbb{G}^l \in \mathbb{F}^l} \mathbb{P}\left(\sum_{e \in \bar{E}_k^l} c_{e,l}\mathrm{y}_e \le H_l\right) \ge 1 - \epsilon_H \tag{16c}$$

$$\inf_{\mathbb{S} \in \mathbb{F}^{\mathcal{A}}} \mathbb{P}\left(\sum_{i \in \bar{V}_k^l} a_i \mathrm{x}_i \le Q_l\right) \ge 1 - \epsilon_Q \tag{16d}$$

$$\sum_{e \in \delta(j)} \mathrm{y}_e = 2\mathrm{x}_j, \ \forall j \in V_k^l \tag{16e}$$

$$\mathrm{x}_i \in \{0,1\}, \ \mathrm{y}_e \in \{0,1\}, \ \forall i \in \bar{V}_k^l, e \in E_k^l \tag{16f}$$

where $\delta^-(i)$ and $\delta^+(i)$ are the set of incoming and outgoing edges to vertex i. Constraints (16b) represent the flow conservation from the source to the target. Problems (10) and (16) differ in two components: the objective functions and constraints (10b) and (16b). The remaining constraints are the same. Let the ordered variables $\mathrm{y}(p) = (\mathrm{y}_{i_0,i_1}, \mathrm{y}_{i_1,i_2}, \cdots, \mathrm{y}_{i_{n_p},i_{n_p+1}})$ be a path in the models provided $\mathrm{y}_{i_\iota,i_\iota+1} = 1$ for $\iota \in \{0,1,...,n_p\}$. To prove the proposition, we will show that a solution in Problem (10) corresponds to a solution in the reformulated shortest path problem, Problem (16), with the same objective value, and vice versa.

Let $\mathrm{y}(p)$ for a feasible path in Problem (16), constructed by path formation constrains (16b), and hold the capacity and travel range constraints, imposed by (16c) and (16d). The path formation constraints (16b) ensure that a path starts from SA k i.e., $i_0 = k$, visits a subset of PoDs in $\bar{V}_k^l$, exactly once i.e., $\nexists i_\iota, i_\nu$ such that $i_\iota, i_\nu \in I_p$, $i_\iota = i_\nu$, and ends at k' i.e., $i_{n_p+1} = k'$. Note that k' is a dummy vertex replicating SA k. Path $\mathrm{y}(p)$ can be exactly constructed by Constraints (10b) as they ensure that a route that starts from SA k, returns to SA k with no subtour. Hence, a route in Problem (10) corresponds to a path in Problem (16). Therefore, for a route in Problem (10) and its corresponding path in Problem (16), $\mathrm{x}^{(10)} = \mathrm{x}^{(16)}$. Regarding the cost for path p, we have

$$\sum_{e \in E_p} \bar{c}_{e,l}\mathrm{y}_e = \sum_{(i,j) \in E_p} \left(\mu_j \beta_k + (\mu_{i,j,l} + \varphi_{j,l})\pi_k^l - \alpha_j(1-\omega_j) - \alpha_j^{\mathcal{D}}\omega_j\right) \mathrm{y}_{i,j}$$

$$= \sum_{j \in I_p} \Big(\mu_j \beta_k + \varphi_{j,l} \pi_k^l - \alpha_j (1-\omega_j) - \alpha_j^{\mathcal{P}} \omega_j \Big) \mathrm{x}_j + \sum_{(i,j) \in E_p} \mu_{i,j,l} \pi_k^l \mathrm{y}_{i,j}$$

The last equation is valid because according to constraint (16e) when $\mathrm{y}_{i_\iota, i_{\iota+1}} = 1$ and $\mathrm{y}_{i_{\iota+1}, i_{\iota+2}} = 1$ for $j = \iota + 1$ then $\mathrm{x}_j = 1$. Note that $\pi_k^l \varpi^l$ is a fixed part of the route reduced cost associated with SA k and mobile unit l. This concludes our proof.

B.2. Deterministic Equivalent derivation for CVaR-based Constraint (13)

Following Uryasev and Rockafellar (2000), we interpret the loss function as resource utilization. Accordingly, we define the VaR and CVaR at a confidence level of $1-\epsilon$ for the capacity constraint by

$$\mathrm{VaR}_\epsilon(\boldsymbol{a}) := \min \Big\{ q \in \mathbb{R} : \mathbb{P}(\boldsymbol{a} \leq q) \geq 1-\epsilon \Big\} \tag{17}$$

$$\mathrm{CVaR}_\epsilon(\boldsymbol{a}) := \mathbb{E}\Big[\boldsymbol{a} \,\Big|\, \boldsymbol{a} \geq \mathrm{VaR}_\epsilon(\boldsymbol{a}) \Big]. \tag{18}$$

Given the additive property of normally distributed random variables (closure under addition) i.e., when $a_i \sim \mathbb{N}(\mu_i, \sigma_i^2)$ then $\boldsymbol{a} \sim \mathbb{N}(\boldsymbol{\mu}, \boldsymbol{\sigma^2})$ where $\boldsymbol{\mu} = \sum_{i \in I_r} \mu_i$ and $\boldsymbol{\sigma}^2 = \sum_{i \in I_r} \sigma_i^2$. Hence, it is trivial that $\mathrm{VaR}_{1-\epsilon}(\boldsymbol{a}) = \boldsymbol{\mu} + \sqrt{\boldsymbol{\sigma^2}} \Phi^{-1}(1-\epsilon)$ provided $\Phi^{-1}(1-\epsilon)$ is the inverse cumulative distribution function of the standard normal distribution at risk level ϵ.

$$\mathbb{E}\Big[\boldsymbol{a} \,\Big|\, \boldsymbol{a} \geq \mathrm{VaR}_{1-\epsilon}(\boldsymbol{a}) \Big] = \frac{1}{\epsilon} \int_{\mathrm{VaR}_{1-\epsilon}(\boldsymbol{a})}^{\infty} \boldsymbol{a} \cdot f_{\boldsymbol{a}}(a) \, d\boldsymbol{a} = \boldsymbol{\mu} + \frac{1}{\epsilon} \sqrt{\boldsymbol{\sigma^2}} \phi(\nu), \tag{19}$$

provided $\phi(\nu)$ is the probability density function of the standard normal distribution $(f_{\boldsymbol{a}})$ for demand $\boldsymbol{a}$ at ν and $\nu = \Phi^{-1}(1-\epsilon) = \frac{\mathrm{VaR}_{1-\epsilon}(\boldsymbol{a}) - \boldsymbol{\mu}}{\sqrt{\boldsymbol{\sigma^2}}}$. The latter results from the fact that we computed the expected value of one-sided truncated normal distribution, leading to the following deterministic counterparts for travel range and capacity constraints:

$$\sum_{(i,j) \in E_p} \mu_{i,j,l} + \frac{\phi(z_{1-\epsilon_H})}{\epsilon_H} \sqrt{\sum_{(i,j) \in E_p} (\sigma_{i,j,l})^2} \leq H_l \;\text{ and }\; \sum_{i \in I_p} \mu_i + \frac{\phi(z_{1-\epsilon_Q})}{\epsilon_Q} \sqrt{\sum_{i \in I_p} (\sigma_i)^2} \leq Q_l. \tag{20}$$

B.3. Proof of Proposition 2

To prove Proposition 2, we restate the distributionally robust chance constraint (8) as:

$$\sup_{\mathbb{G}^l \in \mathbb{F}} \mathbb{P} \left(\sum_{e \in E_r} c_{e,l} \geq H_l \right) \leq \epsilon. \tag{21}$$

Let $c = \{c_{e,l}\}_{|E_r|}$ be the matrix of uncertain travel times in a given route r traversed by mobile unit l. Without loss of generality and for the sake of simplicity, we drop index l. We assume that travel time matrix c belongs to a family of probability distributions with mean vector μ and covariance matrix Λ i.e., $c \sim (\mu, \Lambda)$. The bound for Chebyshev inequality provided by Theorem 6.1 in Bertsimas and Popescu (2005) and Lemma 2.1 in Chen et al. (2011) is computed as follows:

$$\sup_{c \sim (\mu, \Lambda)} \mathbb{P}(c \in S) = \frac{1}{1+d^2}$$

where $S = \{c : \sum_{e \in E_r} c_e > H\}$ and

$$d^2 = \inf_{c \in S} (c-\mu)^T (\Lambda)^{-1} (c-\mu). \tag{22}$$

For simplicity, we introduce a vector of auxiliary random variables ξ and substitute $c-\mu$ with ξ (i.e., $\xi = c-\mu$). So, $\mathbb{E}(\xi) = \mathbb{E}(c) - \mu = 0$ and $Var(\xi) = \mathbb{E}\left[(\xi - \mathbb{E}(\xi))^T (\xi - \mathbb{E}(\xi))\right] = \mathbb{E}\left[(c-\mu)^T (c-\mu)\right]$. Thus, problem (22) is written:

$$d^2 = \inf \quad \xi^T(\Lambda)^{-1}\xi \quad \text{s.t.} \sum_{e\in E_r} \xi_e > H - \sum_{e\in E_r} \mu_e.$$

To solve the above quadratic program (QP), we use the Lagrange method:

$$\mathcal{L}(\xi,\lambda) = \xi^T(\Lambda)^{-1}\xi + \lambda \cdot \Big(\sum_{e\in E_r} \xi_e - H + \sum_{e\in E_r} \mu_e\Big),$$

where λ is the Lagrangian multiplier. The solution to the QP is $d^2 = \frac{(H-\sum_{e\in E_r}\mu_e)^2}{\zeta^T\Lambda\zeta}$ provided $\zeta^T = [1 \, ... \, 1]$. The equation (21) is valid if $\frac{1}{1+d^2} \le \epsilon$. Substituting d^2 into this inequality and rearranging terms results in:

$$\frac{\zeta^T\Lambda\zeta}{\zeta^T\Lambda\zeta + (H - \sum_{e\in E_p}\mu_e)^2} \le \epsilon \implies \sum_{e\in E_r} \mu_e + \sqrt{\frac{1-\epsilon}{\epsilon}\,\zeta^T\Lambda\zeta} \le H. \tag{23}$$

This concludes the proof of the proposition. The same procedure can be extended to obtain a deterministic equivalent of the capacity-related chance constraint.

B.4. Counterexample for the Optimal Substructure Property

The *optimal substructure property* is the fundamental feature of a dynamic programming-based method for standard shortest path problems, i.e., for any optimal path $P^*_{k\to j}$ from source k to vertex j, every subpath $P^*_{k\to i} \subset P^*_{k\to j}$ is itself optimal: $P^*_{k\to j} = P^*_{k\to i} + P^*_{i\to j}$. However, given the probabilistic constraints, the optimal substructure property does not hold in our shortest path problem. We demonstrate this claim by a counterexample. Let $L_1(i) = [10,(34,100),(9,36)]$ and $L_2(i) = [12,(35,32),(10,17)]$ represent the (reduced) cost, the mean and variance of travel time, and the mean and variance of demand for visited vertices, respectively, for two paths $p_1(i)$ and $p_2(i)$, illustrated in Figure B.1.

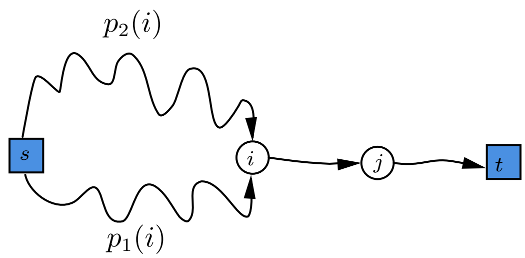

Figure B.1 Optimal substructure in the shortest path problem

Suppose $a_j \sim \mathcal{N}(3,1)$ and $c_{i,j} \sim \mathcal{N}(5,4)$. Since the (reduced) cost of p_1 is smaller, a standard shortest path algorithm will eliminate $p_2(i)$. Let $\epsilon = 0.05$, $z_{0.95} = 1.645$, $H = 50$ and $Q = 20$. Therefore, we need to check if the probabilistic constraints (10c and 10d) for demand and travel time constraints hold. Given normally distributed demand and travel time, $\mu + z_{0.05}\sigma$ for demand and travel time will be compared against Q and H. Table B.1 reports the contribution of the mean and standard deviation of demand and travel time for $p_1(i)$ and $p_2(i)$ when both paths are extended to vertex j. While the standard dynamic programming rule eliminates $p_2(i)$ (keeping $p_1(i)$), it turns out that $p_2(i)$ is feasible and $p_1(i)$ is infeasible. Boldface values in the table indicate the feasible values with respect to $Q = 20$ and $H = 50$.

As the example illustrates, the shortest path from the source s to the target t includes $p_2(i)$, however, the shortest path from the source s to the vertex i is $p_1(i)$. This counterexample shows that the optimal substructure property does not hold under probabilistic constraints.

Table B.1 Mean and standard deviation's contribution probabilistic constraints, an example.

	Demand			Travel time		
	μ	$z_{0.05}\sigma$	$\mu + z_{0.05}\sigma$	μ	$z_{0.05}\sigma$	$\mu + z_{0.05}\sigma$
$p_1(j)$	12.00	10.01	22.01	39.00	16.78	55.78
$p_2(j)$	13.00	6.98	**19.98**	40.00	9.87	**49.87**

B.5. Proof of Proposition 3

As demonstrated by the counterexample in Appendix B.4, unlike conventional shortest path problems, the optimal solution to the underlying problem *does not* consist of optimal solutions to smaller independent subproblems; that is, the optimal substructure property does not hold in our case. With the insight from this example, we introduced conditions (C1-C3) that will ensure the optimally of the proposed dynamic program. To this end, we first define a new notion: *inverse stochastic dominance*. According to the conventional first order stochastic dominance, if $\mathbb{P}_1(\xi_1 \le w) \le \mathbb{P}_2(\xi_2 \le w), \forall w \in \mathbb{R}$, then ξ_1 is first-order stochastic dominant over ξ_2. However, since we are interested in paths with higher probability of validity in our problem, the inverse relationship is defined as follows

Definition 1 (Inverse Stochastic Dominance). *Let $\xi_1 \sim \mathbb{D}_1$, $\xi_2 \sim \mathbb{D}_2$ be random variables with distribution functions $\mathbb{D}_1$ and $\mathbb{D}_2$, respectively. ξ_1 is inverse stochastic dominant over ξ_2 if $\mathbb{P}_1(\xi_1 \ge Q) \le \mathbb{P}_2(\xi_2 \ge Q)$ for $Q \in R$.*

Intuitively, we prefer a random variable if its distribution function has heavier left tail than that of another one. Definition 1 implies that ξ_1 is less likely to violate a constraint compared to ξ_2; thus, we can exclude the path associated with ξ_2 and proceed with the path associated with ξ_1, thereby guaranteeing that Path 2 cannot lead to a better solution than Path 1. Given Definition 1, we prove this proposition for three policies corresponding to normally distributed chance constraints, normally distributed CVaR-based constraints and distributionally robust chance constraints. Let vertices and edges on paths 1 and 2 be presented by I_1, I_2, E_1, and E_2, respectively. Note that both paths 1 and 2 start from SA k and end at vertex i.

Proof for Normally Distributed Chance Constraints. Suppose uncertain travel times and demands follow normal distributions, i.e., $c_{e,l} \sim \mathcal{N}(\mu_{e,l}, \sigma_{e,l}^2)$ and $a_i \sim \mathcal{N}(\mu_i, \sigma_i^2)$. For a given ϵ, Conditions C1 and C2 i.e., $\sum_{j\in I_{p_1}(i,k)} \mu_j \le \sum_{j\in I_{p_2}(i,k)} \mu_j$, $\sum_{j\in I_{p_1}(i,k)} \sigma_j^2 \le \sum_{j\in I_{p_2}(i,k)} \sigma_j^2$, $\sum_{e\in E_{p_1}(i,k)} \mu_{e,l} \le \sum_{e\in E_{p_2}(i,k)} \mu_{e,l}$ and $\sum_{e\in E_{p_1}(i,k)} \sigma_{e,l}^2 \le \sum_{e\in E_{p_2}(i,k)} \sigma_{e,l}^2$ result in

$$\text{Travel range:} \quad \sum_{e\in E_{p_1}} \mu_{e,l} + z_{1-\epsilon_H}\sqrt{\sum_{e\in E_{p_1}} \sigma_{e,l}^2} \le \sum_{e\in E_{p_2}} \mu_{e,l} + z_{1-\epsilon_H}\sqrt{\sum_{e\in E_{p_2}} \sigma_{e,l}^2} \tag{24}$$

$$\text{Capacity:} \quad \sum_{i\in I_{p_1}} \mu_i + z_{1-\epsilon_Q}\sqrt{\sum_{i\in I_{p_1}} \sigma_i^2} \le \sum_{i\in I_{p_2}} \mu_i + z_{1-\epsilon_Q}\sqrt{\sum_{i\in I_{p_2}} \sigma_i^2} \tag{25}$$

According to the deterministic equivalents (12), the above inequalities imply $\mathbb{P}(\sum_{e\in E_{p_1}} c_{e,l} \le H_l) \le \mathbb{P}(\sum_{e\in E_{p_2}} c_{e,l} \le H_l)$ and $\mathbb{P}(\sum_{i\in I_{p_1}} a_i \le Q_l) \le \mathbb{P}(\sum_{i\in I_{p_2}} a_i \le Q_l)$. It is straightforward to verify that when paths 1 and 2 are extended from vertex i to the subsequent vertex j (which may correspond to either a PoD or an SA) in the induced graph G_k^l, the above inequalities remain valid, i.e.,

$$\sum_{e\in E_{p_1}} \mu_{e,l} + \mu_{e',l} + z_{1-\epsilon_H}\sqrt{\sum_{e\in E_{p_1}} \sigma_{e,l}^2 + \sigma_{e',l}^2} \le \sum_{e\in E_{p_2}} \mu_{e,l} + \mu_{e',l} + z_{1-\epsilon_H}\sqrt{\sum_{e\in E_{p_2}} \sigma_{e,l}^2 + \sigma_{e',l}^2} \tag{26}$$

$$\sum_{i\in I_{p_1}} \mu_i + \mu_j + z_{1-\epsilon_Q}\sqrt{\sum_{i\in I_{p_1}} \sigma_i^2 + \sigma_j^2} \le \sum_{i\in I_{p_2}} \mu_i + \mu_j + z_{1-\epsilon_Q}\sqrt{\sum_{i\in I_{p_2}} \sigma_i^2 + \sigma_j^2} \tag{27}$$

where the paths are extended from vertex i to vertex j such that $e' = (i,j)$, the means and variances of travel time for edge e' by mobile unit l and demand for vertex j are denoted by $(\mu_{e',l}, (\sigma_{e',l})^2)$ and (μ_j, σ_j^2), respectively. Note that all means and variances are positive. As can be easily verified, when the paths are extended $\bar{p}_1$ and $\bar{p}_2$, we have $\mathbb{P}(\sum_{e\in E_{\bar{p}_1}} c_{e,l} \leq H_l) \leq \mathbb{P}(\sum_{e\in E_{\bar{p}_2}} c_{e,l} \leq H_l)$ and $\mathbb{P}(\sum_{i\in I_{\bar{p}_1}} a_i \leq Q_l) \leq \mathbb{P}(\sum_{i\in I_{\bar{p}_2}} a_i \leq Q_l)$. Therefore, when Condition C3 holds, i.e., $\bar{c}_{p_1}(i,k,l) \leq \bar{c}_{p_2}(i,k,l)$, path 2 can be safely excluded, as it cannot yield a feasible path with a lower reduced cost than path 1

Proof for Normally Distributed CVaR. Similar to normally distributed chance constraints, suppose uncertain travel time and demand follow normal distributions, i.e., $c_{e,l} \sim \mathcal{N}(\mu_{e,l}, \sigma_{e,l}^2)$ and $a_i \sim \mathcal{N}(\mu_i, \sigma_i^2)$. For a given pre-specified ϵ, Conditions C1 and C2 lead to

$$\text{Travel time:} \quad \sum_{e\in E_{p_1}} \mu_{e,l} + \frac{\phi(z_{1-\epsilon_H})}{\epsilon_H}\sqrt{\sum_{e\in E_{p_1}} \sigma_{e,l}^2} \leq \sum_{e\in E_{p_2}} \mu_{e,l} + \frac{\phi(z_{1-\epsilon_H})}{\epsilon_H}\sqrt{\sum_{e\in E_{p_2}} \sigma_{e,l}^2} \tag{28}$$

$$\text{Demand:} \quad \sum_{i\in I_{p_1}} \mu_i + \frac{\phi(z_{1-\epsilon_Q})}{\epsilon_Q}\sqrt{\sum_{i\in I_{p_1}} \sigma_i^2} \leq \sum_{i\in I_{p_2}} \mu_i + \frac{\phi(z_{1-\epsilon_Q})}{\epsilon_Q}\sqrt{\sum_{i\in I_{p_2}} \sigma_i^2} \tag{29}$$

Based on the deterministic equivalent (13), the above inequalities imply that $\text{CVaR}_{\epsilon_Q}(\sum_{i\in I_{\bar{p}_1}} a_i \ \mathrm{x}_{i,r}) \leq \text{CVaR}_{\epsilon_Q}(\sum_{i\in I_{\bar{p}_2}} a_i \ \mathrm{x}_{i,r})$ and $\text{CVaR}_{\epsilon_H}(\sum_{e\in E_{\bar{p}_1}} c_{e,l} \ \mathrm{y}_{e,r} \leq H_l) \leq \text{CVaR}_{\epsilon_H}(\sum_{e\in E_{\bar{p}_2}} c_{e,l} \ \mathrm{y}_{e,r} \leq H_l)$, where subscripts 1 and 2 denote paths 1 and 2, respectively. Similar to the previous case, when extending paths 1 and 2 from vertex i to vertex j, if Condition C3 holds ($\bar{c}_{p_1}(i,k,l) \leq \bar{c}_{p_2}(i,k,l)$), path 2 can be safely excluded.

Proof for Distributionally Robust Chance Constraints. Let us assume that only the first and second moments of the probability distributions for the travel time and demand are available, when planning decisions are made. For a given pre-specified ϵ, Conditions C1 and C2 yield:

$$\text{Demand:} \quad \sum_{i\in I_{p_1}} \mu_i + \sqrt{\sum_{i\in I_{p_1}} \frac{1-\epsilon}{\epsilon}\sigma_i^2} \leq \sum_{i\in I_{p_2}} \mu_i + \sqrt{\sum_{i\in I_{p_1}} \frac{1-\epsilon}{\epsilon}\sigma_i^2} \tag{30}$$

$$\text{Travel time:} \quad \sum_{e\in E_{p_1}} \mu_{e,l} + \sqrt{\sum_{e\in E_{p_1}} \frac{1-\epsilon}{\epsilon}\sigma_{e,l}^2} \leq \sum_{e\in E_{p_2}} \mu_{e,l} + \sqrt{\sum_{e\in E_{p_1}} \frac{1-\epsilon}{\epsilon}\sigma_{e,l}^2} \tag{31}$$

According to the deterministic equivalents (14), the above inequalities ensure

$$\inf_{\mathbb{G}\in\mathbb{S}} \mathbb{P}\left(\sum_{i\in I_{p_1}(i,k)} a_i \geq Q\right) \leq \inf_{\mathbb{G}\in\mathbb{S}} \mathbb{P}\left(\sum_{i\in I_{p_2}(i,k)} a_i \geq Q\right)$$

$$\inf_{\mathbb{G}\in\mathbb{F}} \mathbb{P}\left(\sum_{e\in E_{p_1}(i,k)} c_e \geq H\right) \leq \inf_{\mathbb{G}\in\mathbb{F}} \mathbb{P}\left(\sum_{e\in E_{p_2}(i,k)} c_e \geq H\right).$$

Similar to normally distributed chance constraints, these conditions guarantee that when paths p_1 and p_2 are extended to vertex j, path p_1 can not become infeasible before path p_2. When Conditions C1-C3 holds, then Path p_2 can be safely excluded. This concludes our proof.

B.6. Development of Valid Inequalities and their Proofs

Integer programs with pure binary variables are known to have weak linear programming relaxation; see Nemhauser and Wolsey (1988) for details. We develop three sets of valid inequalities to strengthen the linear programming relaxation of Problem 1. The objective is to form valid inequalities that do not remove any integer feasible solution and potentially tighten the LP relaxation and improve the convex hull approximation. The first category links the SA location decisions to the mobile unit allocation decisions. The second and third categories of valid inequalities utilize a new set of variables ($u_{i,j}$) to connect route decisions to the SA location and mobile unit allocation decisions, respectively.

PROPOSITION 4. *For any staging area $k \in K$, the following inequalities are valid:*

$$x_{k,d} \leq \sum_{m \in M} y_{k,m}, \forall k \in K, \ \forall d \in D \tag{32a}$$

$$x_{k,t} \leq \sum_{m \in M} y_{k,m}, \forall k \in K, \ \forall t \in T \tag{32b}$$

$$\sum_{m \in M} y_{k,m} \leq \sum_{t \in T} x_{k,t} + \sum_{d \in D} x_{k,d}, \forall k \in K \tag{32c}$$

Proof of Proposition 4. Inequalities (32a-32c) are valid by construction. Mobile units (either drones or trucks) cannot be allocated to a staging area that is not open, i.e., if $\sum_{m \in M} y_{k,m} = 0$, then $x_{k,d} = 0$ and $x_{k,t} = 0$ for all $k \in K$, $d \in D$ and $t \in T$. Moreover, if a mobile unit is located at staging area k, the staging area must be opened. In other words,

$$x_{k,d} \leq \sum_{m \in M} y_{k,m}, \ \forall d, k \ \text{ and } x_{k,t} \leq \sum_{m \in M} y_{k,m}, \ \forall t, k.$$

Conversely, if staging area k is opened, at least one mobile unit needs to be assigned to the staging area, otherwise (i.e., no mobile unit is assigned to the staging area) the staging area will not be used to support the affected areas. Inequality (32c), restated below, ensures staging areas are not idle if they are opened.

$$\textstyle\sum_{m \in M} y_{k,m} \leq \sum_{t \in T} x_{k,t} + \sum_{d \in D} x_{k,d} \quad \forall k.$$

Let $u_{i,j}$ be a new set of binary variables, each of which is equal to 1 if an edge (i, j) is traversed in a route by a mobile unit, and zero otherwise. This new variable $u_{i,j}$ can then be linked to the route decisions as:

$$u_{i,j} = \sum_{d \in D} \sum_{r \in R^d(i,j)} z_{r,d} + \sum_{t \in T} \sum_{r \in R^t(i,j)} z_{r,t}, \forall i, j \in I,$$

where $R^t(i, j)$ ($R^d(i, j)$) is the set of routes traversed by truck t (drone d) that include edge (i, j),$\forall i, j \in I$. Since all PoDs must be visited exactly once, we have $\sum_{i \in V} u_{i,j} = 1$ and $\sum_{i \in V} u_{j,i} = 1$ for all $j \in I$.

PROPOSITION 5. *For each SA k, the below inequalities link variables u to x and are valid:*

$$u_{i,k} \leq \textstyle\sum_{t \in T} x_{k,t} + \sum_{d \in D} x_{k,d}, \forall i \in I, \forall k \in K. \tag{33}$$

Proof of Proposition 5. Given $u_{i,k} = \sum_{d \in D} \sum_{r \in R^d(i,k)} z_{r,d} + \sum_{t \in T} \sum_{r \in R^t(i,k)} z_{r,t}$, $u_{i,k}$ indicates whether there is a direct link between PoD i and SA k. If no mobile unit travels from i to k i.e., $\sum_{t \in T} x_{k,t} + \sum_{d \in D} x_{k,d} = 0$, then there must not be a direct link between PoD i and staging area k i.e., $u_{i,k} = 0$. And if there is a direct link between i and k, some mobile unit must traverse the link i.e., if $u_{i,k} = 1$, then $\sum_{t \in T} x_{k,t} + \sum_{d \in D} x_{k,d} = 1$. The constraint $u_{i,k} \leq \sum_{t \in T} x_{k,t} + \sum_{d \in D} x_{k,d}, \forall i, k$ enforces these two conditions This concludes the proof.

PROPOSITION 6. *For each SA k, the following inequalities link variables u to y and are valid:*

$$u_{i,k} \leq \textstyle\sum_{m \in M} y_{k,m}, \forall i \in I, \forall k \in K. \tag{34}$$

Proof of Proposition 6. If SA k is not open ($\sum_{m \in M} y_{k,m} = 0$), then there should be no link between PoD i and staging area k. However, if a link between PoD i and staging area k is required i.e., $u_{i,k} = 1$, then staging area k must be open. This is indicated by the constraint $u_{i,k} \leq \sum_{m \in M} y_{k,m}, \ \forall i, k$. This concludes the proof.

B.7. Solution Method Overview

We develop a customized B&P algorithm to solve our PDVRP-LFD. Because the pricing problem is central to the efficiency of a B&P algorithm, we focus on its formulation and solution, as described in Section 3. Figure B.2 outlines the overall algorithm, with the highlighted box indicating the role of the pricing problem within it. The branching process is managed by the solver SCIP (available at https://scipopt.org/)

We begin the solution process by solving RMP with an initial set of routes. Based on the dual information from the current solution, we solve the reformulated pricing subproblem (SSPCC) to identify new routes with negative reduced cost that could improve the objective. This step is carried out for each SA and for each individual mobile unit potentially available at the SA. If such routes are found, we add them to the RMP and resolve it. This column generation loop continues iteratively until no further improving routes exist for the current RMP. When the column generation terminates, the solution of the current RMP is checked for integrality. If the solution is integer and its objective value is lower than the previous upper bound (initially set to infinity), we update the global upper bound and keep it as a candidate optimal solution, otherwise, the current solution is discarded. If the solution is fractional, the current solution is branched by introducing additional constraints, for example, fixing certain variable values, and create new child nodes representing subproblems. These nodes are added to the node pool, which stores all pending subproblems generated during the branching process. The procedure is repeated, i.e., a node from the pool is selected, the current RMP is solved, the pricing problem is solved and branching is performed if necessary. When a better integer solution is found, the best known solution is updated. This iterative process continues until the node pool is empty, i.e., all subproblems have been explored or pruned. At that point, the algorithm terminates, and we return the best integer solution found throughout the search.

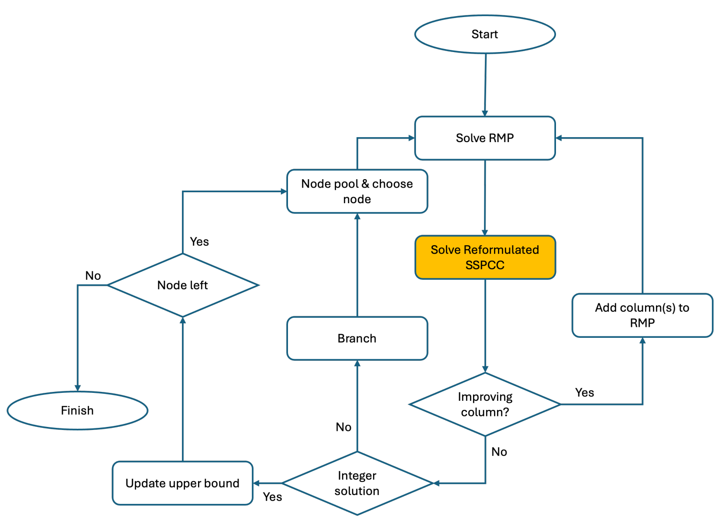

Figure B.2 The main steps of our proposed B&P Algorithm

Appendix C: Additional Details and Results for the Case study

C.1. Case study Description and Motivations

Following Hurricanes Eta and Iota in November 2020, Honduras faced a severe humanitarian crisis, with an estimated 3.9 million people affected and over 368,000 individuals left isolated (IFRC 2021). The storms caused extensive infrastructure damage, including more than 900 roads and 60 bridges, leaving many communities inaccessible for weeks and some for months after the events. In response, the Honduran Red Cross conducted rescue operations and distributed essential supplies, including over 2,800 food kits, 2,100 hygiene kits, and 200,000 liters of water, among others. Despite these efforts, the available truck fleet proved insufficient; thus, the International Federation of Red Cross and Red Crescent Societies (IFRC) supplied three additional trucks and contracted private services to expand delivery capacity (IFRC 2021). We focuses on the Sula Valley region—the largest alluvial valley in Honduras—which was among the most affected areas (Figure C.1). Home to about 20% of the national population and traversed by the Ulúa and Chamelecón rivers, the valley is highly flood-prone, while surrounding mountainous areas face landslides and bridge collapses that isolate communities until infrastructure is restored. We selected this region due to its large number of isolated communities and our direct communication with local contacts who provided first-hand accounts of relief efforts. The network includes PoDs and candidate SAs, as shown in Figure C.1. Activated SAs serve as both departure and return locations for mobile units (trucks and drones). Although allowing mobile units to terminate at different SAs could increase routing flexibility, it would significantly complicate coordination—particularly in resource-limited settings—and require additional infrastructure for loading, battery recharging, and maintenance across multiple SAs, which may be impractical in post-disaster operations.

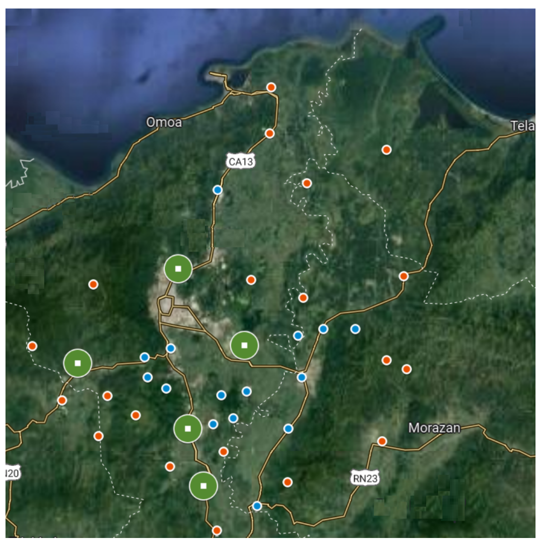

Figure C.1 Potential SAs and PoDs in the Sula Valley region: big green circles indicate PoDs that can also potentially function as SAs, blue circles represent accessible PoDs, and red circles represent isolated PoDs.

C.2. Data Generation and Honduras Case Studies

In addition to the Sula Valley case study, we construct two benchmark sets. **Set 1** includes seven problem sizes with five random instances each. For every instance, we generate PoDs by sampling longitude–latitude coordinates within given bounds using Poisson–disc sampling, which enforces a minimum separation distance to avoid clustering. A subset of SAs is then selected so that each PoD is reachable by both trucks and drones from at least one SA (under mode-specific accessibility constraints).

Travel distances are modeled as follows. Drone travel distance between any two vertices is given by Euclidean distance, $dist^d_{i,j}$. Road distances for trucks are represented as a multiplicative perturbation of

Euclidean distance: $dist^t_{i,j} := \kappa_{i,j} \cdot dist^d_{i,j}$, where $\kappa_{i,j} \sim U[1, 1.8]$. Given constant modal speeds for drones and trucks, mean travel times are directly derived from these distance models. The travel times' standard deviations are assumed proportional to average travel distance as:

$$\bar{\sigma}^d_{i,j} = \eta^d_{i,j} \cdot \bar{\mu}^d_{i,j} \text{ and } \bar{\sigma}^t_{i,j} = \eta^t_{i,j} \cdot \bar{\mu}^t_{i,j}, \text{ where } \eta^d_{i,j}, \eta^t_{i,j} \sim U[0.03, 0.09].$$

We additionally mark a random subset of vertices (excluding SAs) as isolated, meaning that they have no road connections to any other PoDs or SAs. The PoD demand means are then sampled as integers: $a_i \sim \text{UniformInt}[1, 24]$ for non-isolated PoDs, and $a_i \sim \text{UniformInt}[1, 4]$ for isolated PoDs. In both cases, demand uncertainty is introduced via proportional standard deviations: $\sigma_i \sim \theta_i \cdot a_i$, where $\theta_i \sim U[0.01, 0.1]$.

The characteristics of Set 1 are summarized in Table C.1.

Table C.1 The Characteristics of Test Problems

	No. of Potential SAs	No. of PoDs	No. of Isolated PoDs	Longitude Range	Latitude Range
Problem structure 1	3	20	6	U[0,50]	U[0,50]
Problem structure 2	4	25	7	U[0,55]	U[0,55]
Problem structure 3	4	30	8	U[0,60]	U[0,60]
Problem structure 4	4	35	10	U[0,60]	U[0,60]
Problem structure 5	4	40	12	U[0,65]	U[0,65]
Problem structure 6	5	45	14	U[0,65]	U[0,65]
Problem structure 7	5	50	16	U[0,65]	U[0,65]

Set 2 is based on the road network of northern Honduras, divided into six regions. While the Sula Valley serves as the primary case study, the other five regions provide additional synthetic instances. Certain road links, shown as dashed lines in Figure 2, are classified as *disaster-prone* and assumed to fail with 50% probability, reflecting the vulnerability of transportation infrastructure to hurricanes and floods. Disrupted roads in Regions 2–5 are highlighted in red. Road distances between vertices are obtained from Google Maps, while aerial distances use Euclidean metrics. Travel times and PoD demands follow the same generation procedure as in Set 1, with demands scaled to local population estimates. SAs are chosen from major residential centers with robust infrastructure to ensure feasibility as operational hubs. The critical characteristics of the six regions are summarized in Table C.2.

Table C.2 Critical characteristics of different regions of Honduras.

Regions	Area	No. of Potential SAs	No. of Served PoDs	No. of Isolated PoDs
Sula Valley	7,384 km^2	5	35	20
Tela	3,380 km^2	4	23	5
Yoro	3,951 km^2	4	30	10
Arenal	4,619 km^2	4	29	12
Saba	5,391 km^2	5	34	7
San Esteban	12,463 km^2	5	36	20

C.3. Demand Partitioning under Capacity Constraints

Following Proposition 2, in the DR policy, the uncertain demand of individual PoD i, with mean μ_i and standard deviation σ_i, attains its worst-case value W_i as:

$$W_i = \mu_i + \sqrt{\frac{(1-\epsilon)}{\epsilon}}\sigma_i, \text{ where } \epsilon \in (0, 1).$$

If for a given PoD i, the above worst-case demand exceeds the available drone capacity or the minimum capacity of heterogeneous drone fleet, presented by $Q^{D-\min}$, the problem may be infeasible. To maintain feasibility, we partition the PoD into multiple sub-PoDs such that each sub-PoD's worst-case demand is at most $Q^{D-\min}$, while preserving the total worst-case demand. The minimum number of required sub-PoDs is given by $n_i = \left\lceil \frac{W_i}{Q^{D-\min}} \right\rceil$, then we assign the mean and standard deviation demand of each sub-vertex as:

$$\mu_j = \frac{\mu_i}{W_i} W_j,\ \sigma_j = \frac{\sigma_i}{W_i} W_j,\ \text{ for } j = 1, 2, \cdots, n_i,\ \text{ where } W_j = \begin{cases} Q^{D-\min} & \text{for } j = 1, 2, \cdots, n_i - 1, \\ W_i - (n_i - 1) Q^{D-\min}, & \text{for } j = n_i. \end{cases}$$

Through this decomposition, the worst-case demand is distributed across multiple feasible sub-PoDs, ensuring that mobile unit's capacity constraints are never violated. Importantly, the total robust demand as well as the original mean and variance characteristics of the demand distribution are preserved, making the method both consistent and generalizable to any problem instance.

C.4. Allocation of Single-Capacity Drone (Description and Model)

When the drone can only carry one kit at a time, the problem becomes a drone-PoD allocation problem in which a drone will make multiple single-load direct trips to serve each PoD from SAs. Let $w_{i,k,d}$ be a binary variable equal to 1 if drone d is located at SA k and visits PoD i. Let $o_{i,d}$ denote the total loading, return travel and service time for PoD i, i.e., $o_{i,d} = \varpi^{\mathcal{D}} + 2c_{i,k,d} + \varphi_{i,d}$. Note that a PoD may be served by drones from different SAs. This setting is applicable under the assumption that the humanitarian logistics system can coordinate such plans, assignment and operations; otherwise, additional constraints would be needed to allocate each PoD to drones from a single SA. The resulting problem can be formulated as

$$\min \sum_{k \in K} \sum_{d \in D(k)} b^d x_{k,d} \tag{35a}$$

$$\text{s.t.} \sum_{i \in I} o_{i,d} w_{i,k,d} \leq \rho x_{k,d},\ \forall d \in D(k),\ k \in K \tag{35b}$$

$$\sum_{k \in K} \sum_{d \in D(k)} w_{i,k,d} \geq a_i,\ \forall i \in I \tag{35c}$$

$$c_{i,k,d} w_{i,k,d} \leq H_d,\ \forall i \in I,\ d \in D(k),\ k \in K \tag{35d}$$

$$w_{i,k,d} \in \{0,1\}, x_{k,d} \in \{0,1\}, \forall i \in I,\ d \in D(k),\ k \in K. \tag{35e}$$

The objective function (35a) minimizes fixed drone cost. Constraints (35b) state if drone d is located at SA k, then its trips to serve assigned PoDs in total cannot exceed the delivery time limit (ρ). Constraints (35c) ensure sufficient trips are assigned to PoD i to cover its demand. Constraints (35d) avoid allocating a PoD to a drone beyond its travel range. Constraints (35e) ensure the binary restriction on the variables. Under travel time and demand uncertainty, and within the DR policy (Proposition 2), the deterministic equivalents of Constraints (35c) and (35d) are formulated as:

$$\sum_{k \in K} \sum_{d \in D(k)} w_{i,k,d} \geq \mu_i + \sqrt{\frac{1-\epsilon_Q}{\epsilon_Q}} \sigma_i, \text{ and } \left(\mu_{i,k,d} + \sqrt{\frac{1-\epsilon_H}{\epsilon_H}} \sigma_{i,k,d}\right) w_{i,k,d} \leq H^d,\ \forall i \in I,\ d \in D(k),\ k \in K.$$

C.5. Performance Evaluation of Different Policies

In this appendix, we present detailed results for the performance evaluation of different policies on randomly generated synthetic instances. In the tables below, the first column ("instance") specifies the tuple (# of potential SAs, # of PoDs, # of isolated PoDs), while the second column identifies the corresponding generated instance within the problem structure described in Appendix C.2. The remaining columns are explained in

§4.2.1. As in Tables C.3-C.6, the algorithm solved the problems to optimal or near-optimal solutions, with a maximum optimality gap of 7.2%. Specifically, optimal solutions (optimality gap $< 0.05\%$) within the limit of 7,200 seconds were obtained in 30 of 35 DR instances (average CPU time: 1,656s), 30 of 35 CVaR instances (1,589s), 26 of 35 CC instances (1,723s), and 22 of 35 DET instances (1,854s). For the few instances that did not reach optimality within the time limit, the average gaps were 2.56%, 3.66%, 2.83%, and 2.84% for DR, CVaR, CC, and DET, respectively. The largest gaps—6.0%, 5.8%, 7.1%, and 7.2%—were all observed in the largest setting, with five potential SAs, 50 PoDs, and 16 isolated PoDs. The observed gaps occurred mainly in instances with at least 45 PoDs, reflecting the exponential growth in routing combinations.

Table C.3 Distributionally robust policy results

Instance		(NS,ND,NT)	(R_d,R_t)	(NR_d,NR_t)	Obj	G(%)	T(s)	DFT	DFD	TFT	TFD	FTR
(3,20,6)	I	(2,1,3)	(6,6)	(1.2,1.6)	382	0.0	214	0.0%	0.0%	0.0%	0.0%	0.0%
	II	(2,2,3)	(6,6)	(1.5,1.3)	680	0.0	115	0.3%	0.0%	0.0%	0.0%	0.1%
	III	(2,1,4)	(6,8)	(1,1.3)	402	0.0	314	0.0%	0.0%	0.0%	0.0%	0.0%
	IV	(2,1,3)	(5,6)	(1.4,1.7)	382	0.0	216	0.0%	0.0%	0.0%	0.0%	0.0%
	V	(2,2,2)	(8,4)	(1.2,1.7)	662	0.0	322	0.0%	0.0%	0.0%	0.0%	0.0%
(4,25,7)	I	(3,2,5)	(9,9)	(1.1,1.2)	730	0.0	235	0.0%	0.0%	0.0%	0.0%	0.0%
	II	(2,2,2)	(10,4)	(1.3,2)	664	0.0	374	0.0%	0.0%	0.0%	0.0%	0.0%
	III	(3,2,6)	(9,15)	(1.3,1.4)	750	0.0	455	0.0%	0.0%	0.0%	0.0%	0.0%
	IV	(3,2,5)	(8,8)	(1.1,1.5)	730	0.0	512	0.0%	0.0%	0.0%	0.0%	0.0%
	V	(3,2,4)	(7,8)	(1.2,1.5)	712	0.0	264	0.0%	0.0%	0.0%	0.0%	0.0%
(4,30,8)	I	(4,3,6)	(10,12)	(1.1,1.3)	1062	0.0	371	0.0%	0.0%	0.0%	0.0%	0.0%
	II	(3,2,5)	(9,10)	(1.1,1.6)	732	0.0	239	0.0%	0.0%	0.1%	0.0%	0.1%
	III	(4,2,5)	(7,10)	(1.3,1.7)	740	0.0	425	0.0%	0.0%	0.0%	0.0%	0.0%
	IV	(4,2,8)	(11,12)	(1,1.3)	800	0.0	6517	0.0%	0.0%	0.0%	0.0%	0.0%
	V	(4,3,6)	(10,12)	(1,1.3)	1064	0.0	338	0.0%	0.0%	0.0%	0.0%	0.0%
(4,35,10)	I	(3,3,5)	(14,10)	(1.1,1.6)	1032	0.0	248	0.0%	0.0%	0.0%	0.0%	0.0%
	II	(3,2,5)	(10,11)	(1.2,1.7)	736	0.0	481	0.0%	0.0%	0.0%	0.0%	0.0%
	III	(4,3,5)	(13,10)	(1.1,1.7)	1042	0.0	459	0.1%	0.0%	0.0%	0.0%	0.0%
	IV	(4,2,5)	(10,10)	(1.1,2)	742	0.0	281	0.0%	0.0%	0.0%	0.0%	0.0%
	V	(4,2,6)	(11,13)	(1,1.5)	762	0.0	302	0.0%	0.0%	0.0%	0.0%	0.0%
(4,40,12)	I	(3,2,6)	(10,12)	(1.3,1.9)	757	0.0	466	0.0%	0.0%	0.0%	0.0%	0.0%
	II	(3,2,6)	(11,12)	(1.2,1.9)	757	0.0	834	0.0%	0.0%	0.0%	0.0%	0.0%
	III	(3,2,8)	(12,17)	(1.1,1.4)	797	0.0	2096	0.0%	0.0%	0.0%	0.0%	0.0%
	IV	(4,3,7)	(15,12)	(1.3,1.4)	1080	0.0	4914	0.0%	0.0%	0.0%	0.0%	0.0%
	V	(3,3,8)	(14,14)	(1.1,1.4)	1096	0.0	6811	0.2%	0.0%	0.0%	0.0%	0.1%
(5,45,14)	I	(4,2,6)	(11,14)	(1.3,1.9)	764	3.4	7200	0.0%	0.0%	0.0%	0.0%	0.0%
	II	(5,3,6)	(14,11)	(1.4,1.8)	1072	0.0	3290	0.0%	0.0%	0.0%	0.0%	0.0%
	III	(4,3,6)	(13,12)	(1.2,2)	1064	0.0	3859	0.0%	0.0%	0.0%	0.0%	0.0%
	IV	(4,3,6)	(16,11)	(1.2,1.9)	1064	2.0	7200	0.0%	0.0%	0.0%	0.0%	0.0%
	V	(5,3,7)	(14,12)	(1.1,2)	1094	1.2	7200	0.0%	0.0%	0.0%	0.0%	0.0%
(5,50,16)	I	(3,3,9)	(16,14)	(1.2,1.9)	1119	0.2	7200	0.0%	0.0%	0.0%	0.0%	0.0%
	II	(4,3,7)	(15,15)	(1.3,1.7)	1089	0.0	5245	0.3%	0.0%	0.0%	0.0%	0.1%
	III	(4,3,7)	(15,14)	(1.3,1.8)	1086	0.0	4193	0.0%	0.0%	0.0%	0.0%	0.0%
	IV	(4,4,14)	(14,20)	(1.1,1.5)	1527	6.0	7200	0.0%	0.0%	0.0%	0.0%	0.0%
	V	(4,3,7)	(15,14)	(1.5,1.6)	1085	0.0	5303	0.0%	0.0%	0.0%	0.0%	0.0%

C.6. Investment costs in the synthetic instances

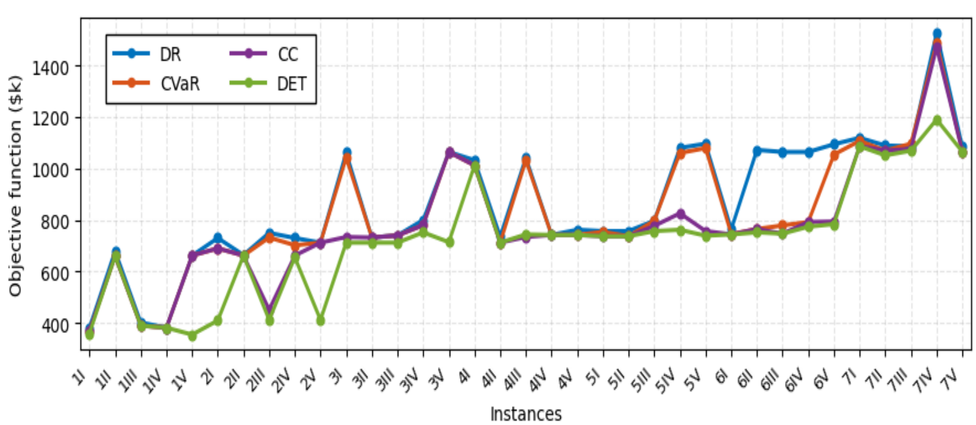

Figure C.2 The behavior of objective functions across all instances derived by each policy.

Table C.4 CVaR policy results

Instance		(NS,ND,NT)	(R_d,R_t)	(NR_d,NR_t)	Obj	G(%)	T(s)	DFT	DFD	TFT	TFD	FTR
	I	(3,1,2)	(5,4)	(1.4,2.5)	370	0.0	256	0.0%	0.0%	0.0%	0.0%	0.0%
	II	(2,2,2)	(7,4)	(1.4,1.7)	660	0.0	312	0.0%	0.0%	0.0%	0.3%	0.1%
(3,20,6)	III	(3,1,3)	(5,5)	(1.4,2)	390	0.0	216	0.0%	0.0%	0.0%	0.0%	0.0%
	IV	(2,1,3)	(5,6)	(1.4,1.6)	382	0.0	318	0.0%	0.0%	0.0%	0.4%	0.1%
	V	(2,2,2)	(8,3)	(1.3,2.3)	662	0.0	217	0.2%	0.1%	0.3%	0.0%	0.2%
	I	(3,2,3)	(8,6)	(1.4,1.7)	690	0.0	221	0.0%	0.1%	0.3%	0.2%	0.1%
	II	(2,2,2)	(9,3)	(1.4,2.6)	662	0.0	1720	0.0%	0.0%	0.0%	0.0%	0.0%
(4,25,7)	III	(3,2,5)	(7,8)	(1.4,1.3)	732	0.0	333	0.0%	0.1%	0.0%	0.0%	0.0%
	IV	(2,2,4)	(9,5)	(1.5,1.4)	702	0.0	516	0.0%	0.1%	0.1%	0.0%	0.0%
	V	(3,2,4)	(7,6)	(1.4,1.8)	712	0.0	215	0.0%	0.1%	0.2%	0.0%	0.1%
	I	(4,3,5)	(10,8)	(1.2,1.7)	1042	0.0	344	0.0%	0.0%	0.1%	1.1%	0.2%
	II	(3,2,5)	(9,8)	(1.3,1.7)	732	0.0	196	0.0%	0.0%	0.1%	0.0%	0.1%
(4,30,8)	III	(4,2,5)	(9,10)	(1.2,1.5)	740	0.0	235	0.0%	0.0%	8.1%	0.0%	3.9%
	IV	(4,2,7)	(10,11)	(1,1.5)	780	0.0	3826	0.0%	0.0%	0.0%	0.0%	0.0%
	V	(4,3,6)	(10,12)	(1,1.3)	1064	0.0	249	0.0%	0.0%	0.0%	0.0%	0.0%
	I	(3,3,4)	(15,8)	(1.1,1.8)	1012	0.0	272	0.0%	0.0%	0.0%	0.1%	0.1%
	II	(3,2,4)	(10,8)	(1.3,2.2)	712	0.0	7071	0.0%	0.9%	0.0%	0.2%	0.8%
(4,35,10)	III	(3,3,5)	(13,8)	(1.2,1.9)	1032	0.0	532	0.2%	0.0%	0.7%	0.0%	0.4%
	IV	(4,2,5)	(8,9)	(1.5,2.1)	742	0.0	291	0.1%	0.0%	0.0%	0.0%	0.1%
	V	(4,2,5)	(9,10)	(1.3,1.9)	742	0.0	390	0.0%	0.0%	0.8%	0.2%	0.9%
	I	(3,2,6)	(10,11)	(1.5,1.9)	754	0.0	1903	0.3%	0.0%	0.0%	0.0%	0.2%
	II	(3,2,5)	(10,11)	(1.5,1.9)	737	0.0	1789	0.0%	0.0%	0.0%	0.0%	0.0%
(4,40,12)	III	(3,2,8)	(11,15)	(1.3,1.7)	797	0.0	6282	0.1%	0.0%	0.1%	0.1%	0.1%
	IV	(4,3,6)	(15,10)	(1.3,1.7)	1060	0.0	1478	0.1%	0.0%	0.0%	0.0%	0.1%
	V	(3,3,7)	(13,14)	(1.2,1.4)	1079	0.0	739	0.2%	0.1%	0.0%	0.0%	0.1%
	I	(4,2,5)	(9,10)	(1.5,2.6)	745	0.0	2378	0.0%	0.0%	2.0%	0.0%	1.0%
	II	(4,2,6)	(8,9)	(2,2.6)	765	4.3	7200	1.4%	0.0%	0.2%	0.0%	1.3%
(5,45,14)	III	(3,2,7)	(10,12)	(1.6,2)	779	2.8	7200	2.7%	0.0%	3.5%	0.0%	3.0%
	IV	(5,2,7)	(10,12)	(1.4,2.2)	792	2.0	7200	2.6%	0.0%	3.3%	0.0%	2.9%
	V	(5,3,5)	(14,10)	(1.4,2)	1054	0.0	3978	0.0%	0.0%	5.0%	0.0%	2.1%
	I	(4,3,8)	(16,13)	(1.1,2.1)	1107	0.0	3062	0.8%	0.0%	0.4%	0.1%	0.7%
	II	(4,3,6)	(16,16)	(1.3,1.6)	1069	0.0	4739	0.4%	0.0%	0.0%	0.1%	0.2%
(5,50,16)	III	(5,3,7)	(15,13)	(1.3,1.9)	1096	3.4	7200	0.1%	0.0%	2.0%	0.1%	1.0%
	IV	(4,4,12)	(18,16)	(1.1,1.6)	1489	5.8	7200	0.0%	0.1%	0.2%	0.0%	0.1%
	V	(4,3,6)	(15,13)	(1.3,1.9)	1065	0.0	3607	0.0%	0.0%	0.0%	0.0%	0.0%

Table C.5 Chance constraint policy results

Instance		(NS,ND,NT)	(R_d,R_t)	(NR_d,NR_t)	Obj	G(%)	T(s)	DFT	DFD	TFT	TFD	FTR
	I	(3,1,2)	(5,4)	(1.4,2.5)	370	0.0	496	0.0%	0.0%	0.0%	0.0%	0.0%
	II	(2,2,2)	(7,3)	(1.6,2)	660	0.0	243	0.1%	0.1%	0.0%	0.1%	0.3%
(3,20,6)	III	(3,1,3)	(5,7)	(1.4,1.4)	390	0.0	354	0.1%	0.1%	0.0%	0.2%	0.2%
	IV	(2,1,3)	(5,6)	(1.6,1.5)	382	0.0	288	0.8%	0.0%	0.2%	0.0%	0.5%
	V	(2,2,2)	(7,3)	(1.4,2.3)	662	0.0	373	0.0%	0.0%	1.0%	0.3%	0.5%
	I	(3,2,3)	(9,5)	(1.3,1.8)	690	0.0	230	0.4%	0.0%	0.2%	0.3%	0.4%
	II	(2,2,2)	(10,4)	(1.4,1.7)	662	0.0	319	0.3%	0.0%	0.0%	0.0%	0.1%
(4,25,7)	III	(3,1,6)	(4,10)	(1.7,1.4)	452	0.0	5439	0.0%	0.0%	0.1%	0.0%	0.1%
	IV	(2,2,2)	(9,3)	(1.8,1.7)	662	0.0	1739	0.0%	0.1%	0.1%	0.0%	0.0%
	V	(3,2,4)	(8,6)	(1.2,1.8)	712	0.0	249	0.0%	0.0%	0.3%	0.0%	0.1%
	I	(3,2,5)	(10,10)	(1.2,1.4)	734	0.0	339	0.0%	0.1%	0.9%	0.3%	1.0%
	II	(3,2,5)	(9,8)	(1.3,1.7)	732	0.0	253	0.0%	0.1%	0.0%	0.1%	0.1%
(4,30,8)	III	(4,2,5)	(9,9)	(1.2,1.7)	740	0.0	262	0.0%	0.1%	11%	0.4%	5.5%
	IV	(4,2,7)	(11,10)	(1.1,1.4)	780	0.0	6149	0.0%	0.0%	0.0%	0.0%	0.0%
	V	(4,3,6)	(12,11)	(1,1.3)	1064	0.0	784	0.0%	0.1%	0.0%	0. 1%	0.1%
	I	(3,3,4)	(14,8)	(1.2,1.8)	1012	0.0	292	0.9%	0.0%	0.0%	0.1%	0.6%
	II	(3,2,4)	(10,8)	(1.3,2.3)	712	0.0	434	0.8%	0.0%	0.2%	0.6%	0.8%
(4,35,10)	III	(3,2,5)	(9,8)	(1.7,2)	734	0.0	6918	1.2%	0.0%	0.7%	0.0%	1.1%
	IV	(4,2,5)	(9,9)	(1.3,2.1)	742	0.0	257	0.9%	0.0%	0.0%	0.0%	0.4%
	V	(4,2,5)	(9,10)	(1.3,1.9)	742	0.0	391	0.0%	0.0%	0.2%	1.2%	0.9%
	I	(3,2,5)	(10,10)	(1.5,2.1)	737	0.0	2126	0.0%	0.0%	0.0%	0.4%	0.2%
	II	(3,2,5)	(10,9)	(1.5,2.3)	737	0.0	1680	0.0%	0.1%	0.0%	0.4%	0.3%
(4,40,12)	III	(3,2,7)	(11,13)	(1.3,1.6)	777	0.6	7200	0.1%	13.7%	0.1%	0.0%	6.4%
	IV	(4,2,9)	(9,10)	(1.6,2.2)	826	1.5	7200	0.0%	0.0%	0.3%	0.0%	0.1%
	V	(3,2,6)	(9,11)	(1.6,2)	757	0.5	7200	0.1%	0.1%	6.7%	0.0%	3.1%
	I	(4,2,5)	(10,12)	(1.5,2.1)	744	0.0	1572	0.0%	0.0%	3.7%	0.4%	2.1%
	II	(4,2,6)	(8,9)	(2,2.7)	765	3.3	7200	3.0%	0.0%	3.3%	0.0%	3.2%
(5,45,14)	III	(4,2,5)	(10,8)	(1.7,2.9)	747	3.2	7200	2.4%	0.0%	4.8%	0.1%	3.5%
	IV	(5,2,7)	(10,12)	(1.4,2.2)	792	4.0	7200	2.0%	0.1%	3.9%	0.0%	3.0%
	V	(5,2,7)	(10,12)	(1.7,1.9)	794	1.2	7200	0.0%	0.0%	4.9%	0.0%	2.6%
	I	(4,3,7)	(16,15)	(1.2,1.7)	1087	0.0	4128	1.9%	0.0%	0.3%	0.1%	1.2%
	II	(4,3,6)	(14,13)	(1.3,2.1)	1069	4.1	7200	14.3%	0.1%	2.4%	0.2%	8.7%
(5,50,16)	III	(5,3,6)	(16,13)	(1.3,1.9)	1076	0.0	5623	0.0%	0.0%	0.2%	0.1%	0.2%
	IV	(4,4,11)	(18,16)	(1.1,1.6)	1469	0.0	3869	0.0%	0.1%	0.9%	0.1%	0.5%
	V	(4,3,6)	(14,12)	(1.6,1.9)	1065	7.1	7200	0.0%	0.0%	0.0%	0.1%	0.1%

Table C.6 Deterministic policy results

Instance		(NS,ND,NT)	(R_d,R_t)	(NR_d,NR_t)	Obj	G(%)	T(s)	DFT	DFD	TFT	TFD	FTR
(3,20,6)	I	(2,1,2)	(5,5)	(1.8,1.6)	360	0.0	220	0.0%	30%	0.0%	2%	16%
	II	(2,2,2)	(7,4)	(1.4,1.7)	660	0.0	339	0.4%	21%	0.0%	0.3%	13%
	III	(3,1,3)	(5,5)	(1.4,2)	390	0.0	256	0.1%	0.1%	0.0%	0.0%	0.1%
	IV	(2,1,3)	(4,5)	(1.7,2)	382	0.0	298	0.0%	24%	19%	2%	23%
	V	(1,1,2)	(5,4)	(1.4,2.5)	355	0.0	369	0.8%	20%	3%	1%	14%
(4,25,7)	I	(3,1,4)	(5,8)	(1.8,1.5)	410	0.0	454	0.0%	20%	0.0%	10%	17%
	II	(2,2,2)	(9,4)	(1.7,1.5)	662	0.0	362	28%	34%	0.0%	0.0%	43%
	III	(3,1,4)	(5,7)	(1.8,1.7)	412	0.0	5732	40%	10%	17%	0.0%	31%
	IV	(1,2,2)	(7,3)	(2.1,2)	655	0.0	3852	0.0%	20%	7%	0.0%	12%
	V	(3,1,4)	(4,7)	(2,1.9)	412	0.0	5418	36%	13%	0.0%	0.0%	18%
(4,30,8)	I	(3,2,4)	(10,7)	(1.4,1.7)	712	0.0	464	0.0%	20%	1%	3%	14%
	II	(3,2,4)	(10,8)	(1.5,1.4)	712	0.0	358	0.0%	35%	8%	0.0%	23%
	III	(3,2,4)	(8,7)	(1.6,1.9)	712	0.0	356	0.0%	44%	16%	0.0%	31%
	IV	(3,2,6)	(10,9)	(1.4,1.3)	752	0.0	4371	0.0%	31%	1%	3%	18%
	V	(3,2,4)	(9,8)	(1.3,1.8)	714	0.0	651	22%	28%	8%	1%	31%
(4,35,10)	I	(3,3,4)	(14,8)	(1.4,1.5)	1012	0.0	335	1.1%	18.2%	0.0%	0.1%	12.3%
	II	(3,2,4)	(9,8)	(1.4,2.3)	712	0.0	6629	24.5%	21.7%	2.6%	0.0%	25.7%
	III	(4,2,5)	(10,9)	(1.4,1.9)	744	0.0	433	0.5%	5.1%	5.2%	0.1%	5.5%
	IV	(4,2,4)	(8,8)	(1.6,2.3)	742	0.0	597	1.1%	19.2%	0.3%	1.4%	11.0%
	V	(4,2,5)	(8,9)	(1.6,2)	742	0.0	391	0.5%	22.9%	0.1%	0.7%	13.6%
(4,40,12)	I	(3,2,5)	(9,9)	(1.8,2.2)	737	2.7	7200	0.8%	22.3%	2.9%	3.4%	14.7%
	II	(3,2,5)	(10,10)	(1.5,2.1)	737	0.3	7200	0.7%	14.6%	0.0%	3.3%	9.2%
	III	(3,2,6)	(9,9)	(1.8,2.2)	757	0.6	7200	27.2%	31.4%	14.8%	0.5%	36.9%
	IV	(4,2,6)	(10,11)	(1.4,2)	762	0.0	2658	1.1%	5.2%	11.9%	0.0%	9.3%
	V	(3,2,5)	(8,8)	(2,2.5)	739	0.4	7200	13.1%	37.5%	27.6%	2.3%	40.2%
(5,45,14)	I	(4,2,5)	(9,9)	(1.8,2.7)	744	3.8	7200	0.3%	16.8%	17.1%	4.1%	19.2%
	II	(5,2,5)	(10,10)	(1.8,2.2)	752	5.7	7200	10.9%	15.0%	11.5%	3.5%	20.5%
	III	(4,2,5)	(9,10)	(1.9,2.3)	747	4.4	7200	11.4%	11.1%	8.3%	0.9%	15.5%
	IV	(5,2,6)	(10,11)	(1.5,2.3)	774	3.5	7200	0.1%	10.1%	9.1%	7.5%	13.6%
	V	(4,2,7)	(8,10)	(1.9,2.5)	784	1.2	7200	27.6%	36.0%	10.8%	0.1%	34.3%
(5,50,16)	I	(4,3,7)	(14,14)	(1.4,1.9)	1086	2.5	7200	4.8%	19.9%	7.4%	0.1%	16.1%
	II	(4,3,5)	(12,10)	(1.7,2.5)	1051	3.5	7200	23.3%	16.3%	1.4%	4.9%	24.4%
	III	(4,3,6)	(16,11)	(1.4,2)	1069	0.0	6266	0.6%	24.6%	1.7%	12.8%	20.8%
	IV	(4,3,12)	(15,16)	(1.3,1.6)	1190	1.1	7200	2.4%	6.7%	0.2%	3.5%	6.3%
	V	(4,3,6)	(13,10)	(1.7,2.3)	1065	7.2	7200	17.3%	22.4%	7.2%	3.3%	27.0%

C.7. Figures for Evaluation of Different Policies

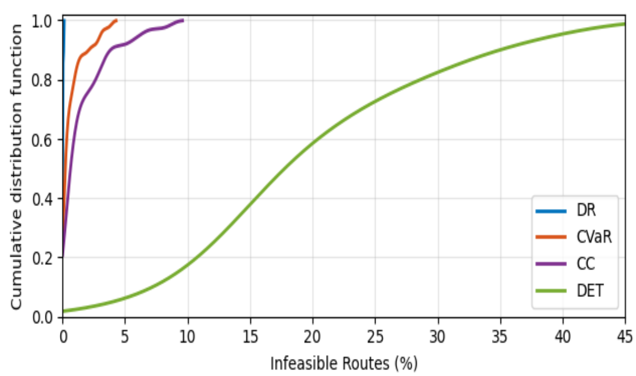

Figure C.3 Smoothed CDFs for the % infeasible route in each policy.

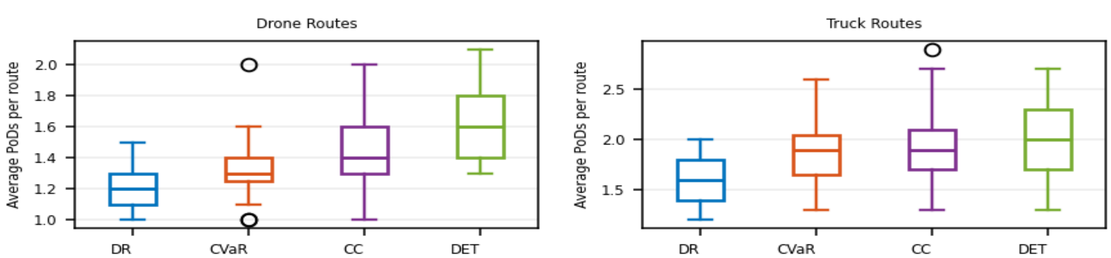

Figure C.4 Average numbers of PoDs per route for both drone & truck under each policy (35 instances).

C.8. Impacts of Isolated PoDs on Policy Performance

We study how the varying number of isolated PoDs affects policy performance by generating five instance classes with different isolation levels in Sula Valley (Table C.7). Investment costs rise substantially across all policies as isolation rises. This underscores the role of *isolated communities* in shaping mobile-unit acquisition, network configuration, and investment needs for effective relief operations. As these communities are inaccessible to conventional trucks, using drones or other aerial units becomes critical despite their high costs. These highlight the importance of optimizing fleet-sizing via the integration of allocation and routing, as the cost of aerial units is substantial relative to other components of post-disaster last-mile humanitarian networks, particularly in resource-limited countries, e.g., Honduras, where such assets are scarce.

Table C.7 **Performance evaluation of different policies in terms of the number of isolated PoDs.**

Policy	Problem	(NS,ND,NT)	(R_d,R_t)	(NR_d,NR_t)	Obj
DR	5I	(2,1,5)	(7,10)	(1.2,2.7)	424
	10I	(2,2,4)	(13,7)	(1.3,2.6)	704
	15I	(2,2,4)	(13,8)	(1.2,2.4)	704
	20I	(2,3,3)	(20,5)	(1.2,2.1)	984
	25I	(2,3,3)	(21,5)	(1.2,2)	984
CvaR	5I	(2,1,5)	(6,10)	(1.3,2.7)	424
	10I	(2,2,4)	(12,7)	(1.4,2.6)	704
	15I	(2,2,3)	(13,6)	(1.4,2.8)	684
	20I	(2,3,3)	(18,6)	(1.3,2)	984
	25I	(3,3,2)	(20,4)	(1.3,2.3)	974
CC	5I	(2,1,5)	(6,10)	(1.3,2.8)	424
	10I	(2,1,5)	(7,10)	(1.4,2.5)	442
	15I	(2,2,3)	(12,7)	(1.4,2.6)	684
	20I	(2,2,3)	(14,6)	(1.4,2.6)	684
	25I	(2,3,2)	(20,5)	(1.3,2)	964
DET	5I	(2,1,4)	(7,9)	(1.4,2.8)	407
	10I	(2,1,5)	(8,10)	(1.4,2.4)	425
	15I	(2,2,3)	(12,7)	(1.4,2.6)	684
	20I	(2,2,3)	(14,6)	(1.5,2.3)	684
	25I	(2,3,2)	(20,5)	(1.3,2)	964

C.9. Choice of ϵ under Shortage Cost Considerations

Figure C.5 shows the interaction between ϵ and the shortage cost for Sula Valley. The pointwise minimum envelope shows a single breakpoint at the intersection of the cost lines corresponding to $\epsilon = 0.30$ and $\epsilon = 0.05$. This breakpoint marks the shortage cost level at which the preferred robustness level shifts: when the shortage cost is low, $\epsilon = 0.30$ yields the lowest total cost, whereas beyond this threshold, $\epsilon = 0.05$ becomes the optimal choice. As the shortage cost increases, policies with smaller ϵ—that is, more conservative and robust decisions—become increasingly preferable.

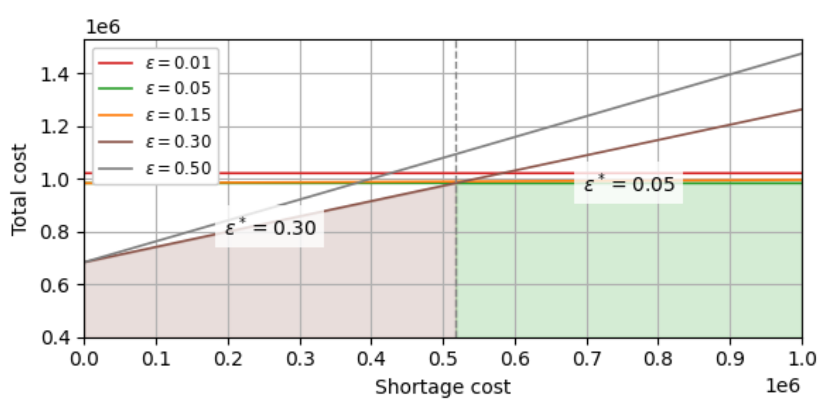

Figure C.5 **Total costs with respect to the shortage cost: optimal ϵ choice.**

References for Appendix

Belenguer JM, Benavent E, Prins C, Prodhon C, Calvo RW (2011) A branch-and-cut method for the capacitated location-routing problem. *Computers & Operations Research* 38(6):931–941.

Bertsimas D, Popescu I (2005) Optimal inequalities in probability theory: A convex optimization approach. *SIAM Journal on Optimization* 15(3):780–804.

Çalık H, Oulamara A, Prodhon C, Salhi S (2021) The electric location-routing problem with heterogeneous fleet: Formulation and benders decomposition approach. *Computers & Operations Research* 131:105251.

Chauhan D, Unnikrishnan A, Figliozzi M (2019) Maximum coverage capacitated facility location problem with range constrained drones. *Transportation Research Part C: Emerging Technologies* 99:1–18.

Chauhan DR, Unnikrishnan A, Figliozzi M, Boyles SD (2021) Robust maximum coverage facility location problem with drones considering uncertainties in battery availability and consumption. *Transportation Research Record* 2675(2):25–39.

Contardo C, Cordeau JF, Gendron B (2013) A computational comparison of flow formulations for the capacitated location-routing problem. *Discrete Optimization* 10(4):263–295.

Contardo C, Cordeau JF, Gendron B (2014) An exact algorithm based on cut-and-column generation for the capacitated location-routing problem. *INFORMS Journal on Computing* 26(1):88–102.

Dukkanci O, Koberstein A, Kara BY (2023) Drones for relief logistics under uncertainty after an earthquake. *European Journal of Operational Research* 310(1):117–132.

Faiz TI, Vogiatzis C, Noor-E-Alam M (2024) Computational approaches for solving two-echelon vehicle and uav routing problems for post-disaster humanitarian operations. *Expert Systems with Applications* 237:121473.

Farham MS, Süral H, Iyigun C (2018) A column generation approach for the location-routing problem with time windows. *Computers & Operations Research* 90:249–263.

Gentili M, Mirchandani PB, Agnetis A, Ghelichi Z (2022) Locating platforms and scheduling a fleet of drones for emergency delivery of perishable items. *Computers & Industrial Engineering* 168:108057.

Ghelichi Z, Gentili M, Mirchandani PB (2022) Drone logistics for uncertain demand of disaster-impacted populations. *Transportation research part C: emerging technologies* 141:103735.

Khameneh RT, Ghorbani-Renani N, Ramirez-Marquez JE (2025) Multi-objective optimization of a truck-drone delivery system for fair and efficient humanitarian logistics under disruption and disinformation. *Computers & Industrial Engineering* 111786.

Kim D, Lee K, Moon I (2019) Stochastic facility location model for drones considering uncertain flight distance. *Annals of Operations Research* 283(1):1283–1302.

Lu Y, Yang J, Yang C (2023) A humanitarian vehicle routing problem synchronized with drones in time-varying weather conditions. *Computers & Industrial Engineering* 184:109563.

Macias JE, Angeloudis P, Ochieng W (2020) Optimal hub selection for rapid medical deliveries using unmanned aerial vehicles. *Transportation Research Part C: Emerging Technologies* 110:56–80.

Mohamed IB, Klibi W, Sadykov R, Şen H, Vanderbeck F (2023) The two-echelon stochastic multi-period capacitated location-routing problem. *European Journal of Operational Research* 306(2):645–667.

Nemhauser G, Wolsey L (1988) *Integer and combinatorial optimization* (Wiley).

Rabta B, Wankmüller C, Reiner G (2018) A drone fleet model for last-mile distribution in disaster relief operations. *International Journal of Disaster Risk Reduction* 28:107–112.

Shadlou MS, Ranjbar M, Salari M (2023) A logic-based benders decomposition algorithm for a repair crew routing and drone scheduling problem after a natural disaster. *Computers & Industrial Engineering* 183:109542.

Sun W, Wu L, Zhang F (2026) An exact algorithm to solve vehicle routing problem with drones for delivery and surveillance tasks after disasters. *Transportation Science* .

Van Steenbergen R, Mes M, Van Heeswijk W (2023) Reinforcement learning for humanitarian relief distribution with trucks and uavs under travel time uncertainty. *Transportation Research Part C: Emerging Technologies* 157:104401.

Wang M, Zhang C, Bell MG, Miao L (2022) A branch-and-price algorithm for location-routing problems with pick-up stations in the last-mile distribution system. *European Journal of Operational Research* 303(3):1258–1276.

Wang S, Sun W, Baldacci R, Elomri A (2025) Exact solution of location–routing problems with heterogeneous fleet and weight-based carbon emissions. *Transportation Research Part E: Logistics and Transportation Review* 193:103862.

Xin X, Wang S, Zhang T (2025) Truck-drone supported humanitarian relief logistics network design: A two-stage distributionally robust optimization approach. *Transportation Research Part C: Emerging Technologies* 178:105231.

Yang Y, Li C, Wang D, Yin Y, Cheng T (2026) A two-stage adaptive robust optimization model for the location-routing problem with drone delivery and uncertainty in humanitarian relief. *Transportation Research Part E: Logistics and Transportation Review* 207:104601.

Yin Y, Yang Y, Yu Y, Wang D, Cheng T (2023) Robust vehicle routing with drones under uncertain demands and truck travel times in humanitarian logistics. *Transportation Research Part B: Methodological* 174:102781.

Zhu T, Boyles SD, Unnikrishnan A (2022) Two-stage robust facility location problem with drones. *Transportation Research Part C: Emerging Technologies* 137:103563.